



# Gastrointestinal tumor-related perihepatic fluorouracil encapsulated lesions and liver metastases: a diagnostic imaging study based on contrast-enhanced computed tomography and magnetic resonance imaging

Yuanqiu Li<sup>1</sup>, Kangwen He<sup>1</sup>, Xinyueyuan Hao<sup>1</sup>, John N. Morelli<sup>2</sup>, Yaqi Shen<sup>1</sup>, Xuemei Hu<sup>1</sup>, Daoyu Hu<sup>1</sup>, Zhen Li<sup>1</sup>

<sup>1</sup>Department of Radiology, Tongji Hospital, Tongji Medical College, Huazhong University of Science and Technology, Wuhan, China; <sup>2</sup>Department of Radiology, St. John's Medical Center, Tulsa, OK, USA

**Contributions:** (I) Conception and design: Y Shen, Y Li; (II) Administrative support: D Hu, Z Li; (III) Provision of study materials or patients: X Hao, X Hu; (IV) Collection and assembly of data: Y Li, K He; (V) Data analysis and interpretation: Y Li, JN Morelli; (VI) Manuscript writing: All authors; (VII) Final approval of manuscript: All authors.

**Correspondence to:** Yaqi Shen, MD, PhD. Department of Radiology, Tongji Hospital, Tongji Medical College, Huazhong University of Science and Technology, 1095 Jiefang Avenue, Qiaokou District, Wuhan 430030, China. Email: yqshen@hust.edu.cn.

**Background:** Perihepatic fluorouracil encapsulated lesions (FELs) can result in potentially confusing computed tomography (CT) and magnetic resonance imaging (MRI) features in postoperative examinations of gastrointestinal tumors. This retrospective study aimed to summarize the typical imaging features of FELs and determine the best imaging modality to distinguish FELs from liver metastases for junior residents.

**Methods:** Patients with FELs who had undergone gastrointestinal tumor surgery in Tongji Hospital from January 2016 to June 2022 were evaluated. The imaging features of FELs were summarized by two senior radiologists. Contrast-enhanced CT (CECT) was used as the primary follow-up tool for postoperative gastrointestinal tumor patients. Patients with FELs and available CECT and MRI examinations were matched with patients with liver metastases based on gender and age and presented in chronological order in a 2:1 ratio. Different imaging modality combinations were used for further evaluation, including a CECT group (modality I), CECT and nonenhanced MRI group (modality II) and CECT with all MRI sequences group (modality III). Subsequently, two junior residents blindly evaluated three groups following a 4-week interval based on a 5-point scale (1= definite benign lesion, 2= probable benign lesion, 3= indeterminate, 4= probable liver metastasis, 5= definite liver metastasis).

**Results:** Imaging features of 33 patients with 36 FELs were analyzed. CECT and dynamic contrast-enhanced MRI (DCE-MRI) showed no enhancement in most lesions. Additionally, 20 patients with FELs meeting the requirements were matched with 40 patients with liver metastases. The highest sensitivity, specificity, and consistency for identifying liver metastases were achieved using a combination of CECT and MRI encompassing all sequences yielded, including modality I (reader 1: 72.0% and 17.4%; reader 2: 62.0% and 17.4%; kappa value 0.295), modality II (reader 1: 88.0% and 8.7%; reader 2: 92.0% and 34.8%; kappa value 0.259), and modality III (reader 1: 98.0% and 34.8%; reader 2: 92.0% and 39.1%; kappa value 0.680).

**Conclusions:** FELs are typically non-enhancing lesions. In our study, two junior residents could best distinguish FELs from liver metastases using CECT with all MRI sequences.

**Keywords:** Fluorouracil implant; computed tomography (CT); magnetic resonance imaging (MRI); diagnosis

Submitted Nov 26, 2022. Accepted for publication Aug 10, 2023. Published online Aug 28, 2023.

doi: 10.21037/qims-22-1315

**View this article at:** <https://dx.doi.org/10.21037/qims-22-1315>

## Introduction

Liver metastasis is a common cause of morbidity and mortality in patients with gastrointestinal cancer. Gastrointestinal cancers tend to metastasize to the liver through its rich portal vein circulation (1). In an analysis of metastasis in 7,559 patients with gastric cancer (2), the liver was the most common site of metastasis (48%). In another study of 5,772 patients with colorectal cancer (3), 1,426 (24.7%) patients developed liver metastases. The relevant guidelines (4,5) recommend aggressive the treatment of liver metastasis based on the number and location of metastases. Treatments include radiotherapy, radiofrequency ablation, systemic therapy, surgical resection, and intraperitoneal administration or implantation of chemotherapy, such as fluorouracil (FU) implants.

FU, introduced in 1958, is a pyrimidine analogue widely used in the treatment of gastrointestinal tumors (6-8). However, FU involves a few toxic side effects including hematologic side effects, gastrointestinal toxicity, and severe bone marrow depression (9). Moreover, the half-life (8–14 minutes) of FU is short, and a rapid metabolism results in decreased plasma levels (10). The severe systemic toxicity and extremely brief plasma half-life of the drug make it particularly suitable for administration through local delivery systems that provide sustained release (11). An *in vitro* study using colon adenocarcinoma cells showed that a lethal dose 50% of continuous infusion of 5-FU was approximately 100 times lower than that administered in a pulsatile manner (12). In addition, it was reported that a continuous infusion of FU demonstrated higher therapeutic efficacy and minimal side effects compared with the bolus injection (13,14).

With respect to FU implants, perihepatic placement can lead to confusing imaging features that share characteristics with liver metastases. Without a multidisciplinary team (MDT) discussion concerning the nature of such lesions, oncologists and surgeons can easily be misled by radiological findings and potentially erroneous reporting, leading to unnecessary additional treatment. Two previous case reports described fluorouracil encapsulated lesion (FEL) being misdiagnosed as a liver tumor, after which surgical resection was performed (15,16). However, the imaging characteristics of FELs have not been characterized or compared with those of liver metastases in a systematic manner.

We therefore conducted a retrospective analysis of the patients with FELs surrounding liver. The purpose of

this study was to characterize the typical imaging features of FELs and determine the optimal imaging modalities necessary for junior residents to successfully distinguish between FELs and liver metastases. We present this article in accordance with the STARD reporting checklist (available at <https://qims.amegroups.com/article/view/10.21037/qims-22-1315/rc>).

## Methods

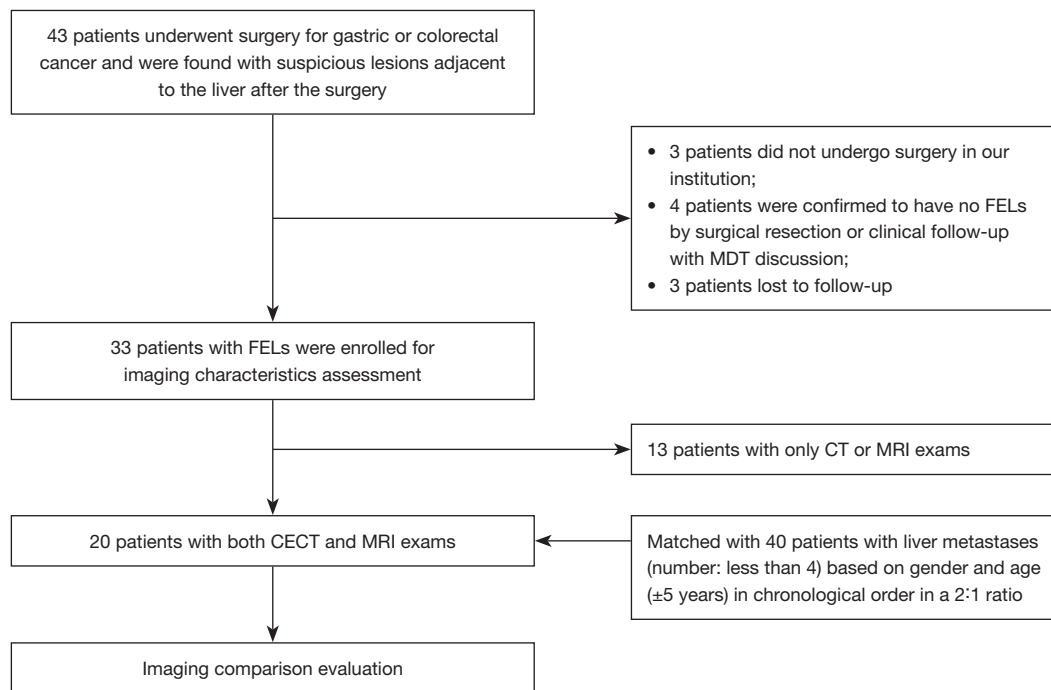
### *Patients and imaging analysis*

This study was conducted in accordance with the Declaration of Helsinki (as revised in 2013) and was reviewed and approved by the Ethics Committee of Tongji Hospital, Tongji Medical College, Huazhong University of Science and Technology. Due to the retrospective retrieval of patient data in this study, informed consent was waived. A systematic review of the electronic medical record system in Tongji Hospital was performed from January 2016 to June 2022 to search for the patients who met the study requirements mentioned below.

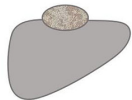
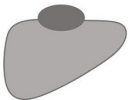
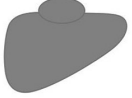
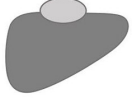
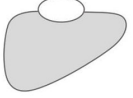
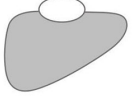
A 2-step analysis was performed: in the first step, two senior radiologists from the MDT team reviewed and summarized the image features of patients with pathological and/or clinical confirmation of FEL; in the second step, two junior radiologists blindly evaluated the images of patients with FELs and those of matched patients with liver metastases. The study flowchart is presented in *Figure 1*.

For imaging characteristic assessment, the inclusion criteria were as follows: (I) patients who underwent surgery for gastric or colorectal cancer and (II) FELs that were found adjacent to the liver on CT or MRI after the surgery and confirmed by surgical resection or clinical follow-up with MDT discussion. The exclusion criteria were as follows: (I) surgery was not performed in our institution and (II) patients lost to follow-up. Serial imaging exams (beginning with initial postoperative CT and/or MRI) of each patient were evaluated independently by two senior radiologists through consensus. The items evaluated included location, number, shape, longest diameter, density (on CT), signal characteristics on T1/T2-weighted imaging (T1/T2WI), diffusion-weighted imaging (DWI) (B=1,000), and enhancement pattern. The features of MRI were represented schematically (*Figure 2*).

Contrast-enhanced CT (CECT) serves as the primary follow-up tool for postoperative gastrointestinal tumor patients. Therefore, for the second part of the study,



**Figure 1** The flowchart of the study. FEL, fluorouracil encapsulated lesion; MDT, multidisciplinary team; CT, computed tomography; MRI, magnetic resonance imaging; CECT, contrast-enhanced computed tomography.

MRI sequence	Type of signal on each image			
T1WI	 Mixed intensity	 Hypointensity		
T2WI	 Mixed intensity	 Hypointensity	 Isointensity	 Mild hyperintensity
DWI	 Isointensity	 Mild hyperintensity	 Hyperintensity	
DCE-MRI	 No enhancement (Arterial phase)	 Enhancement (Portal phase)	 Enhancement (Delayed phase)	

**Figure 2** The schematic of FELs in MRI. The oval part represents the FEL. The intensity of color corresponds to the intensity of the signal. FEL, fluorouracil encapsulated lesion; MRI, magnetic resonance imaging; T1WI, T1-weighted imaging; T2WI, T2-weighted imaging; DWI, diffusion-weighted imaging; DCE-MRI, dynamic contrast-enhanced magnetic resonance imaging.

patients with FELs with both CECT and MRI examination were enrolled. Patients with FELs were matched to those with liver metastases in a 2:1 ratio in chronological order based on gender and age ( $\pm 5$  years). The three diagnostic criteria for patients with liver metastases were as follows: criterion 1 was patients with a history of malignant tumor; criterion 2 was CT or MR imaging features including ring enhancement, intratumoral attenuation or a signal pattern related to possible necrosis cystic degeneration and hemorrhage, or peritumoral attenuation or a signal pattern related to edema; and criterion 3 was pathological confirmation. A diagnosis of liver metastases was made for patients meeting criteria 1 and 2; 1 and 3; or 1, 2, and 3. Patients with more than 3 liver metastases were not included because the number of lesions strongly implied metastases.

Images were evaluated for the presence of liver metastasis. Each imaging evaluation was performed with the different modalities available. Modality I was CECT only, modality II was CECT and nonenhanced MRI, and modality III was CECT and all MRI sequences. Each evaluation was separated by 4 weeks. Two junior residents were asked to separately score each liver lesion on a 5-point Likert-like scale according to the confidence of malignancy (1= definite benign lesion, 2= probable benign lesion, 3= indeterminate, 4= probable liver metastasis, 5= definite liver metastasis). FELs scoring 1 or 2 represented correct identification. Liver metastases scoring 4 or 5 represented correct identification. Junior residents were also asked to document the number of confirmed cysts, hemangiomas, and angiomyolipomas. Patients with more than 5 lesions were recorded as 5 for simplicity.

### *Imaging technique*

Abdominal CECT and MRI scans were performed in accordance with the Liver Imaging Reporting and Data System (LI-RADS; 2018 version). The contrast agent used for CECT was iopromide (370 mg/mL, Ultravist 370; Bayer Schering Pharma, Berlin, Germany). The contrast agent was injected intravenously at a rate of 3.5 mL/s, which was followed by a 20-mL saline flush. The total volume of contrast agent was calculated according to the body weight at 1.5 mL/kg, the reconstruction thickness of CT scan was 1/1.25 mm, the CT tube voltage was 100/120 kVp based on body weight, and the automatically controlled tube current ranged from 100 to 760 mAs. Dynamic contrast-enhanced MRI (DCE-MRI) was performed after a rapid bolus

injection of MultiHance (Bracco Imaging, Milan, Italy) at a rate of 2.5 mL/s, which was immediately followed by a 30-mL saline flush. The total volume of contrast agent was calculated according to the body weight at 0.1 mmol/kg. The CT and MR scanner systems used included the following: Brilliance iCT 256 (Philips Healthcare, Amsterdam, the Netherlands), Aquilion One (Toshiba Medical Systems, Tokyo, Japan), uMR570 (United Imaging Healthcare, Shanghai, China), MAGNETOM Skyra (Siemens Healthineers, Erlangen, Germany), Discovery CT750 (GE HealthCare, Chicago, IL, USA), and Brivo MR 360 (GE HealthCare).

### *Statistical analysis*

Counts and percentages are used to describe categorical variables, while the average age of the patients is expressed using mean  $\pm$  standard deviation (SD). The Student *t*-test was used to compare the mean age between the patients with FELs and those with liver metastases. Weighted kappa statistics were used to assess the agreement between the two junior residents, with the strength of agreement was defined as follows:  $\leq 0.20$ , slight agreement; 0.21–0.40, fair agreement; 0.41–0.60, moderate agreement; 0.61–0.80, good agreement; and  $> 0.80$ , excellent agreement. The sensitivity, specificity, and accuracy for differentiating FELs and liver metastases, including their corresponding 95% confidence intervals (CIs), were calculated for each modality. Positive and negative predictive values were not computed due to the scoring system defining a score of 3 as indeterminate. The Cochran Q test was used to evaluate the differences in identification efficiency among the three modalities. If a significant difference was found ( $P < 0.05$ ), the McNemar test was used for post hoc analysis (Bonferroni correction was adopted with corrected  $P = 0.05/3 \approx 0.017$ ).

## **Results**

### *Clinical characteristics of patients with FELs*

The clinical information of all patients is shown in [Table S1](#). In this retrospective study, a total of 33 (mean age  $55.73 \pm 10.10$  years, range 30–81 years) patients with 36 FELs were included based on the predefined inclusion criteria and exclusion criteria. There were three types of cancers: gastric cancer ( $n=28$ ), colon cancer ( $n=4$ ), and rectal cancer ( $n=1$ ).

FELs were pathologically confirmed in two patients: one

**Table 1** Radiological findings of all FELs

Radiological findings	No. (%) of FELs/mean $\pm$ SD
Location (n=36)	
Adjacent to the left lobe	24 (66.7)
Adjacent to the right lobe	12 (33.3)
Shape (n=36)	
Oval	35 (97.2)
Irregular	1 (2.8)
Longest diameter (millimeter)	21.16 $\pm$ 3.53
Density (n=35)	
Mixed density	22 (62.9)
Isodensity	7 (20.0)
Hyperdensity	6 (17.1)
CECT (n=34)	
Enhancement	0
T1WI (n=25)	
Mixed intensity	9 (36.0)
Hypointensity	16 (64.0)
T2WI (n=25)	
Mixed intensity	11 (44.0)
Hypointensity	2 (8.0)
Isointensity	4 (16.0)
Mild hyperintensity	8 (32.0)
DWI (n=25)	
Isointensity	17 (68.0)
Mild hyperintensity	7 (28.0)
Hyperintensity	1 (4.0)
DCE-MRI (n=24)	
Enhancement	1 (4.2) (portal and delayed phases)

FEL, fluorouracil encapsulated lesion; SD, standard deviation; CECT, contrast-enhanced computed tomography; T1WI, T1-weighted imaging; T2WI, T2-weighted imaging; DWI, diffusion-weighted imaging; DCE-MRI, dynamic contrast-enhanced magnetic resonance imaging.

with colon cancer and the other with rectal cancer. The remaining FELs were clinically confirmed via follow-up imaging and agreement of the MDT. In the patients with pathologically confirmed FELs, one showed necrosis of massive tissue wrapping by fibrous connective tissue

with focal calcification. The other presented with cystic changes and a fibrous capsule. Multinuclear giant cells were also found. No tumor cells were observed in the two pathologically confirmed FELs.

### *Imaging features of all FELs*

Various imaging features of the FELs were evaluated, with results shown in *Table 1* and *Figure 3*. There were 30 patients with 1 FEL and 3 patients with 2 FELs. The FELs were mainly adjacent to the left lobe of the liver (66.7%). A CT scan was available for 35 FELs, revealing 22 FELs with mixed density (3 of which demonstrated cyclic calcification), 7 with isodensity, and 6 with hyperdensity. CECT was available for 34 lesions, but no enhancement was found in the FELs. For noncontrast MRI, 25 lesions were evaluated and found to have the following features: for T1WI, there was hypointensity (n=16) and mixed intensity (n=9); for T2WI, there was hypointensity (n=2), isointensity (n=4), mild hyperintensity (n=8), and mixed intensity (n=11); and for DWI (B=1,000), there was isointensity (n=17), mild hyperintensity (n=7), and hyperintensity (n=1). DCE-MRI was available for 24 lesions, with all but 1 lesion being non-enhancing in the portal phase and delayed phase (*Figure 4*).

### *Evaluation results of the two junior residents*

A total of 20 patients (16 males; 4 females) with FELs met the requirements and were matched with 40 patients with liver metastases. Clinical details for the liver metastasis group are provided in *Table 2* and *Table S2*. The mean age of the groups did not differ (FEL group: 57.90 $\pm$ 8.98 years; liver metastasis group: 58.03 $\pm$ 9.12 years; P=0.96). Among the patients examined for comparison purposes, the total number of cysts, hemangiomas, and angiomyolipomas was 115. No FELs or liver metastases were mistaken for the benign lesions mentioned above. Detailed scores of the two readers based on the 4 modalities are shown in *Table 3*. The concordance of the two readers was fair, fair, and good for modality I (kappa value 0.295), II (kappa value 0.259), and III (kappa value 0.680), respectively. For identifying FELs (n=23) and liver metastases (n=50), the sensitivity and specificity of modality III (reader 1: 98.0% and 34.8%; reader 2: 92.0% and 39.1%) was higher than those of modality I and modality II (*Table 4*). A significant difference in the identification efficiency among the three modalities was found in the two readers (both readers P<0.001). The

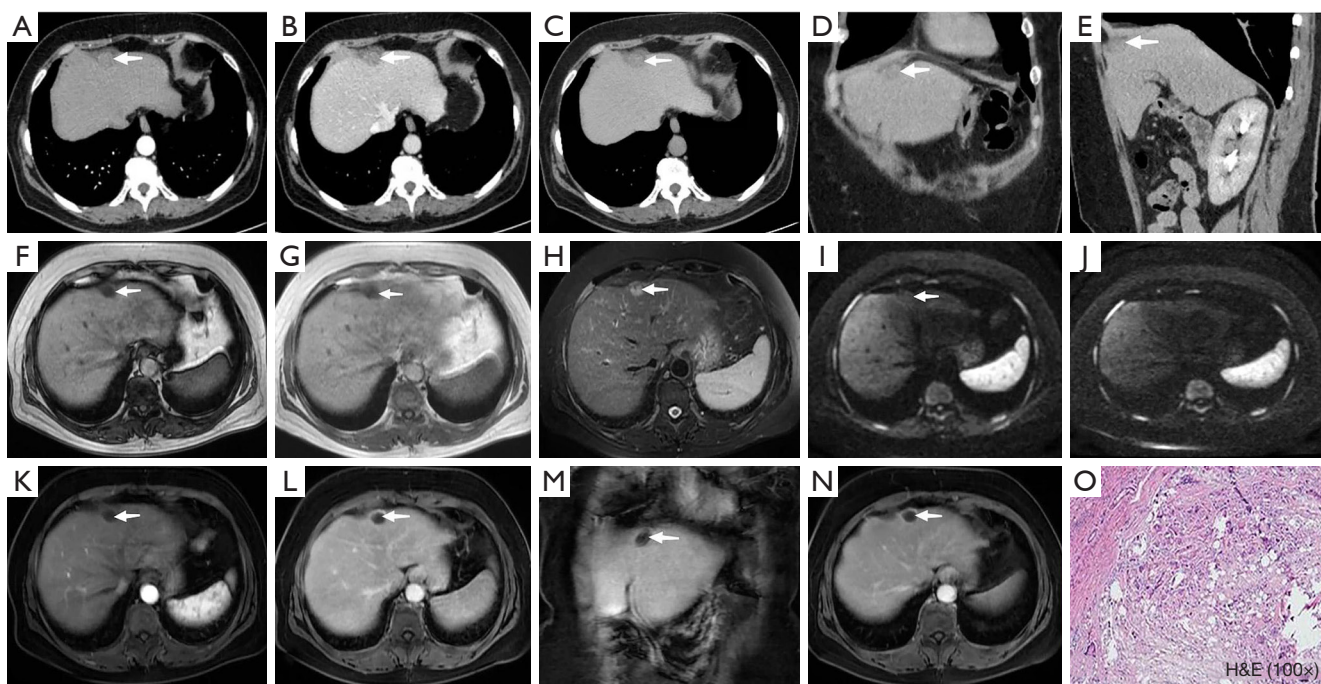


**Figure 3** A series of images from a 58-year-old female who underwent total mesorectal excision. Histopathology showed moderately differentiation adenocarcinoma (pT4N0M0) of the rectum. CECT was performed 1 month after the surgery and revealed a new lesion around the liver. An MRI examination was performed 4 months later. After MDT team discussion, the possibility of a nonmalignant lesion was considered. Finally, surgery was performed to remove the lesion. It proved not to be a liver metastasis via pathology. The white arrow indicates the location of the FEL. (A-E) CECT showed a round, mixed-density lesion with no obvious enhancement. (F,G) In-phase and out-of-phase T1WI showed a hypointensity lesion. (H) T2WI showed a mild hyperintensity lesion. (I) An isointensity lesion was found on DWI (B=600). (J) When the B value increased (B=1,000), the lesion could be not clearly seen. (K-N) DCE-MRI found no obvious enhancement. (O) H&E staining of the tissue demonstrated cystic change but no tumor cells. pTNM, pathological tumor-node-metastasis; CECT, contrast-enhanced computed tomography; MRI, magnetic resonance imaging; MDT, multidisciplinary team; FEL, fluorouracil encapsulated lesion; T1WI, T1-weighted imaging; T2WI, T2-weighted imaging; DWI, diffusion-weighted imaging; DCE-MRI, dynamic contrast-enhanced magnetic resonance imaging; H&E, hematoxylin and eosin.

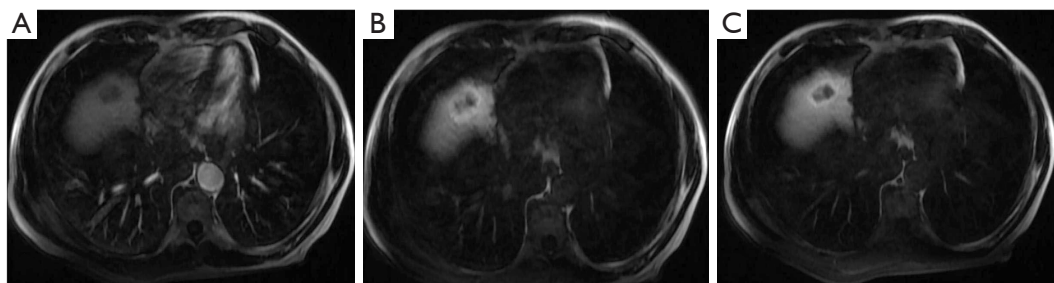


**Figure 4** Enhancement pattern of FEL on DCE-MRI. A 64-year-old male underwent laparoscopic radical resection of the right colon due to colon cancer. Histopathological examination showed poorly differentiated adenocarcinoma (pT2N1M0), and CECT showed a new lesion 1 month after the surgery. To further clarify the nature of the lesion, MRI was performed 3 days later. No enhancement was found in the arterial phase (A). In the portal phase (B) and delayed phase (C), inhomogenous enhancement was found. FEL, fluorouracil encapsulated lesion; DCE-MRI, dynamic contrast-enhanced magnetic resonance imaging; pTNM, pathological tumor-node-metastasis; CECT, contrast-enhanced computed tomography; MRI, magnetic resonance imaging.

**Table 2** Clinical characteristics of the patients for distinguishing FELs and liver metastases

Item	Number of enrolled patients/mean $\pm$ SD		P value
	FEL group (n=20)	Liver metastasis group (n=40)	
Age (years)			
Mean $\pm$ SD	57.90 $\pm$ 8.98	58.03 $\pm$ 9.12	0.96
Range	46–81	43–84	
Male (mean $\pm$ SD, range)	58.75 $\pm$ 9.83, 46–81	58.59 $\pm$ 9.98, 43–84	0.96
Female (mean $\pm$ SD, range)	54.50 $\pm$ 2.89, 51–58	55.75 $\pm$ 3.96, 51–62	0.59
Sex (male/female)	16/4	32/8	
Cancer			
Gastric cancer	17	3	
pTNM			
II	7 (T3N0M0, T3N1M0, T4aN0M0)		
III	10 (T2N3aM0, T3N2M0, T3N3aM0, T4aN3aM0, T4bN2M0)		
Colorectal cancer	3	24	
pTNM			
II	2 (T4N0M0)		
III	1 (T2N1M0)		
Other cancers	0	13	

pTNM staging of gastric cancer and colorectal cancer refers to the Union for International Cancer Control (UICC) and American Joint Committee on Cancer (AJCC) staging system. The TNM staging of patients with liver metastasis is shown in [Table S2](#). FEL, fluorouracil encapsulated lesions; SD, standard deviation; pTNM, pathological tumor-node-metastasis.

**Table 3** Diagnostic scores of 2 readers based on the 3 modalities for distinguishing FELs from metastases

Score	Number of liver metastases						Number of FELs					
	Modality I		Modality II		Modality III		Modality I		Modality II		Modality III	
	Reader 1	Reader 2	Reader 1	Reader 2	Reader 1	Reader 2	Reader 1	Reader 2	Reader 1	Reader 2	Reader 1	Reader 2
1	0	0	0	0	0	0	0	2	0	0	0	2
2	5	4	1	2	0	2	4	2	2	8	8	7
3	9	15	5	2	1	2	8	13	13	8	3	4
4	35	31	40	19	4	6	11	5	8	5	7	4
5	1	0	4	27	45	40	0	1	0	2	5	6

Modality I, CECT; modality II, CECT and non-enhanced MRI; modality III, CECT with all MRI sequences. FEL, fluorouracil encapsulated lesion; CECT, contrast-enhanced computed tomography; MRI, magnetic resonance imaging.

results of the post hoc analysis are shown in [Table 4](#).

## Discussion

The vast majority of FELs examined in this study did not

enhance on CECT or DCE-MRI. For the junior residents, CECT with all MRI sequences resulted in the highest accuracy in identifying liver metastasis and FEL. All but two FELs were confirmed via MDT discussion after the radiologists had identified the lesions.

**Table 4** Summary of the liver metastasis detection performance of the 3 modalities

Detection performance	Reader 1			Reader 2		
	Modality I	Modality II	Modality III	Modality I	Modality II	Modality III
Sensitivity (%)						
Value	72.0 (36/50)	88.0 (44/50)	98.0 (49/50)	62.0 (31/50)	92.0 (46/50)	92.0 (46/50)
95% CI	59.55, 84.45	78.99, 97.01	94.12, 101.88	48.55, 75.45	84.48, 99.52	84.48, 99.52
Specificity (%)						
Value	17.4 (4/23)	8.7 (2/23)	34.8 (8/23)	17.4 (4/23)	34.8 (8/23)	39.1 (9/23)
95% CI	1.90, 32.88	-2.82, 20.21	15.32, 54.25	1.90, 32.88	15.32, 54.25	19.18, 59.08
Accuracy (%)						
Value	54.8 (40/73)	63.0 (46/73)	78.1 (57/73)	47.9 (35/73)	74.0 (54/73)	75.3 (55/73)
95% CI	43.38, 66.21	51.94, 74.09	68.59, 87.57	36.48, 59.41	63.91, 84.04	65.45, 85.23
P value	0.15 (I and II)	0.003 (II and III)	<0.001 (I and III)	<0.001 (I and II)	>0.99 (II and III)	<0.001 (I and III)

Corrected  $P < 0.017$  represents a significant difference. Modality I, CECT; modality II, CECT and non-enhanced MRI; modality III, CECT with all MRI sequences. CI, confidence interval; CECT, contrast-enhanced computed tomography; MRI, magnetic resonance imaging.

FU, an antimetabolite drug, is a common antitumor treatment for gastric and colorectal cancer. Due to its severe side effects and short plasma half-life, a novel delivery method was modified for clinical application. Intraperitoneal chemotherapy, which was proposed in the early 1990s, involves the encapsulation of antitumor drugs in preparation to achieve sustained and efficient drug concentration in local tissues, thereby reducing systemic adverse reactions. Many studies had been devoted to the preparation of FU loading materials to achieve better therapeutic effect (17-19). Leelakanok *et al.* formulated injectable pellets made from poly (lactide co-glycolide) (PLGA) and achieved the sustained release of 5-FU *in vitro* and *in vivo* settings for 1 month, concluding that 5-FU-loaded PLGA pellets were more effective and specifically less erythrototoxic than 5-FU bolus injections (19). Some physicians thus wrap FU with biodegradable adhesion membrane in suspected areas during surgery. However, therapy induced imaging features such as FELs surrounding the liver can be confused for malignancy in oncologic patients. It is thus critical for radiologists and oncologists to understand the imaging features of FEL and to noninvasively distinguish them from those of metastasis.

Most FELs are oval and found adjacent to the left lobe of the liver, which may be related to the habits of surgeons. The density of FELs in present study varied, but most (62.9%) were of mixed density. CECT is used for routine review after resection for malignancy and can generally

distinguish FELs from metastases because FELs show no enhancement. However, cases with atypical imaging findings can be difficult and are not uncommon. In this study, the accuracy of CECT alone was not high (54.8% for reader 1 and 47.9% for reader 2). Prior studies have reported similar difficulties. Shen *et al.* reported that an FEL implanted in the abdomen for adjuvant chemotherapy was misdiagnosed as liver metastasis in a patient with colon cancer (16). In another case report (15), FEL put surrounding the liver during the resection of gastric adenocarcinoma was mistaken for a liver tumor. In those two case reports, no enhancement was found on CECT, which was consistent with the findings of our study. Unfortunately, in both cases, the FELs were misdiagnosed as hepatic tumors and only recognized as benign lesions upon pathologic evaluation.

In this study, the MRI features of FELs were further evaluated. It has been reported in many studies and guidelines that MRI is superior to CT in detecting focal liver lesions, especially in detecting minor liver lesions (20-22). In contrast to liver metastases, which typically restrict diffusion, only 1 FEL was hyperintensity on DWI and 17 FELs were isointensity. Abdominal DWI is unfortunately prone to artifacts, particularly with respect to motion and susceptibility artifacts encountered at air-tissue interfaces between the lung and liver (23). The fact that FELs in this study were all found near the diaphragm might have degraded the DWI assessment. Although the addition of noncontrast

MRI to CECT significantly improved reader 2's ability to distinguish FELs from metastases ( $P < 0.001$ ), the number of correctly diagnosed FELs actually decreased by 2 when nonenhanced MRI was added to CECT for reader 1. Features of benign and malignant tumors overlap on DWI (24) and other unenhanced MRI sequences, and thus lesion characterization should always be completed in combination with unenhanced and DCE-MRI (23). As expected, the additional contrast-enhanced sequences improved lesion characterization for both readers. Only 1 FEL was enhanced in the portal venous and delayed phases, and this might have actually been pseudoenhancement related to the compression of the adjacent liver by the FEL. Statistically, reader 1 showed significant difference in accuracy between modality II and III ( $P = 0.003$ ), and the accuracy of modality I and III differed for both readers ( $P < 0.001$ ;  $P < 0.001$ ). The concordance of the two readers was best with modality III (kappa value 0.680). With the addition of exams and MRI sequences, the number of lesions with a score of 3 decreased, allowing us to conclude that CECT and MRI using all sequences enables optimal distinction between FELs and metastases.

These results also highlight the differences between the imaging appearance of FELs and typical liver metastases. Often the discovery of a new perihepatic lesion following surgery may lead to the presumption of metastatic disease and thus further treatment as per clinical guidelines. Due to limited awareness of FELs, young residents find it challenging to make accurate diagnoses, resulting in the study's low specificity (not exceeding 40%). Even experienced senior radiologists may hesitate to confidently diagnose lesions as questionable for metastasis due to their lack of familiarity with FELs. In current practice, MDT discussions are typically used in the management of patients with cancer to improve prognosis (25,26). Although MDT discussions are routine at our institutions, there were still two patients in this series who underwent early reoperation for suspected metastases that were ultimately FELs. In both cases, pathology showed the FEL encased by fibrous connective tissue. Bai *et al.* (15) similarly described a resected FEL mass as a granuloma with tissue necrosis, surrounded by proliferative fibrous tissue. Such descriptions reflect expected foreign body reactions, which include acute inflammation, chronic inflammation, granulation tissue development, foreign body reaction, and fibrosis/fibrous capsule development (27,28).

There are some limitations to this study. First, the number of patients with FELs was small, and only a cross-sectional study was performed. A further longitudinal

study on the appearance of FELs could be constructive for understanding if and how these lesions evolve over time. Second, the specificity of the three modalities in this study was low, but this emphasizes the crucial need to recognize the existence of FELs. Additionally, the lack of alignment between disease types and stages in patients with liver metastases and those with FELs might have influenced the accuracy of identification.

## Conclusions

FELs are typically non-enhancing perihepatic lesions. In this study, junior residents were able to distinguish FELs from liver metastases. The ability to distinguish FELs from liver metastasis was significantly improved when CECT was used in combination with multiparametric MRI as compared to CECT alone.

## Acknowledgments

We are grateful to the hepatobiliary surgeon, Tianyin Shao (Tongji Hospital, Wuhan) for his assistance in the literature review.

*Funding:* This work was supported by the Teaching Program of Huazhong University of Science and Technology (No. 2022MS045).

## Footnote

*Reporting Checklist:* The authors have completed the STARD reporting checklist. Available at <https://qims.amegroups.com/article/view/10.21037/qims-22-1315/rc>

*Conflicts of Interest:* All authors have completed the ICMJE uniform disclosure form (available at <https://qims.amegroups.com/article/view/10.21037/qims-22-1315/coif>). The authors have no conflicts of interest to declare.

*Ethical Statement:* The authors are accountable for all aspects of the work in ensuring that questions related to the accuracy or integrity of any part of the work are appropriately investigated and resolved. This study was conducted in accordance with the Declaration of Helsinki (as revised in 2013) and was reviewed and approved by the Ethics Committee of Tongji Hospital, Tongji Medical College, Huazhong University of Science and Technology. Due to the retrospective nature of this study, informed consent from patients was waived.

*Open Access Statement:* This is an Open Access article distributed in accordance with the Creative Commons Attribution-NonCommercial-NoDerivs 4.0 International License (CC BY-NC-ND 4.0), which permits the non-commercial replication and distribution of the article with the strict proviso that no changes or edits are made and the original work is properly cited (including links to both the formal publication through the relevant DOI and the license). See: <https://creativecommons.org/licenses/by-nc-nd/4.0/>.

## References

1. Tsilimigras DI, Brodt P, Clavien PA, Muschel RJ, D'Angelica MI, Endo I, Parks RW, Doyle M, de Santibañes E, Pawlik TM. Liver metastases. *Nat Rev Dis Primers* 2021;7:27.
2. Riihimäki M, Hemminki A, Sundquist K, Sundquist J, Hemminki K. Metastatic spread in patients with gastric cancer. *Oncotarget* 2016;7:52307-16.
3. Hackl C, Neumann P, Gerken M, Loss M, Klinkhammer-Schalke M, Schlitt HJ. Treatment of colorectal liver metastases in Germany: a ten-year population-based analysis of 5772 cases of primary colorectal adenocarcinoma. *BMC Cancer* 2014;14:810.
4. Van Cutsem E, Cervantes A, Adam R, Sobrero A, Van Krieken JH, Aderka D, et al. ESMO consensus guidelines for the management of patients with metastatic colorectal cancer. *Ann Oncol* 2016;27:1386-422.
5. Benson AB, Venook AP, Al-Hawary MM, Arain MA, Chen YJ, Ciombor KK, et al. Colon Cancer, Version 2.2021, NCCN Clinical Practice Guidelines in Oncology. *J Natl Compr Canc Netw* 2021;19:329-59.
6. Ilson DH. Esophageal cancer chemotherapy: recent advances. *Gastrointest Cancer Res* 2008;2:85-92.
7. Sexton RE, Al Hallak MN, Diab M, Azmi AS. Gastric cancer: a comprehensive review of current and future treatment strategies. *Cancer Metastasis Rev* 2020;39:1179-203.
8. Vodenkova S, Buchler T, Cervena K, Veskrnova V, Vodicka P, Vymetalkova V. 5-fluorouracil and other fluoropyrimidines in colorectal cancer: Past, present and future. *Pharmacol Ther* 2020;206:107447.
9. Khan S, Aamir MN, Madni A, Jan N, Khan A, Jabar A, Shah H, Rahim MA, Ali A. Lipid poly ( $\epsilon$ -caprolactone) hybrid nanoparticles of 5-fluorouracil for sustained release and enhanced anticancer efficacy. *Life Sci* 2021;284:119909.
10. Grem JL. 5-Fluorouracil: forty-plus and still ticking. A review of its preclinical and clinical development. *Invest New Drugs* 2000;18:299-313.
11. Jung YS, Koo DH, Yang JY, Lee HY, Park JH, Park JH. Peri-tumor administration of 5-fluorouracil sol-gel using a hollow microneedle for treatment of gastric cancer. *Drug Deliv* 2018;25:872-9.
12. Peters GJ, Lankelma J, Kok RM, Noordhuis P, van Groenigen CJ, van der Wilt CL, Meyer S, Pinedo HM. Prolonged retention of high concentrations of 5-fluorouracil in human and murine tumors as compared with plasma. *Cancer Chemother Pharmacol* 1993;31:269-76.
13. Piedbois P, Rougier P, Buyse M, Pignon J, Ryan L, Hansen R, Zee B, Weirnerman B, Pater J, Leichman C, Macdonald J, Benedetti J, Lokich J, Fryer J, Brufman G, Isacson R, Laplanche A, Levy E. Efficacy of intravenous continuous infusion of fluorouracil compared with bolus administration in advanced colorectal cancer. *J Clin Oncol* 1998;16:301-8.
14. Ajani JA, Javle M, Eng C, Fogelman D, Smith J, Anderson B, Zhang C, Iizuka K. Phase I study of DFP-11207, a novel oral fluoropyrimidine with reasonable AUC and low C(max) and improved tolerability, in patients with solid tumors. *Invest New Drugs* 2020;38:1763-73.
15. Bai DS, Jin SJ, He R, Jiang GQ, Yao J. Granuloma induced by sustained-release fluorouracil implants misdiagnosed as a hepatic tumor: A case report. *Oncol Lett* 2014;8:742-4.
16. Shen YY, Qin HW, Zhang JB, Wang ZD, Li P, Pang K, Zhang B, Li S, Cui K. Fluorouracil implants caused a diaphragmatic tumor to be misdiagnosed as liver metastasis: a case report. *BMC Cancer* 2016;16:754.
17. Kasiński A, Zielińska-Pisklak M, Oledzka E, Nałęcz-Jawecki G, Drobniewska A, Sobczak M. Hydrogels Based on Poly(Ether-Ester)s as Highly Controlled 5-Fluorouracil Delivery Systems-Synthesis and Characterization. *Materials (Basel)* 2020;14:98.
18. Ren X, Zheng N, Gao Y, Chen T, Lu W. Biodegradable three-dimension micro-device delivering 5-fluorouracil in tumor bearing mice. *Drug Deliv* 2012;19:36-44.
19. Leelakanok N, Geary SM, Salem AK. Antitumor Efficacy and Toxicity of 5-Fluorouracil-Loaded Poly(Lactide Co-glycolide) Pellets. *J Pharm Sci* 2018;107:690-7.
20. Lee KH, Lee JM, Park JH, Kim JH, Park HS, Yu MH, Yoon JH, Han JK, Choi BI. MR imaging in patients with suspected liver metastases: value of liver-specific contrast agent gadoxetic acid. *Korean J Radiol* 2013;14:894-904.
21. Kim HJ, Lee SS, Byun JH, Kim JC, Yu CS, Park SH,

- Kim AY, Ha HK. Incremental value of liver MR imaging in patients with potentially curable colorectal hepatic metastasis detected at CT: a prospective comparison of diffusion-weighted imaging, gadoxetic acid-enhanced MR imaging, and a combination of both MR techniques. *Radiology* 2015;274:712-22.
22. European Association for the Study of the Liver. Electronic address: easloffice@easloffice.eu; European Association for the Study of the Liver. EASL Clinical Practice Guidelines: Management of hepatocellular carcinoma. *J Hepatol* 2018;69:182-236. Erratum in: *J Hepatol* 2019;70:817.
  23. Lincke T, Zech CJ. Liver metastases: Detection and staging. *Eur J Radiol* 2017;97:76-82.
  24. Kandpal H, Sharma R, Madhusudhan KS, Kapoor KS. Respiratory-triggered versus breath-hold diffusion-weighted MRI of liver lesions: comparison of image quality and apparent diffusion coefficient values. *AJR Am J Roentgenol* 2009;192:915-22.
  25. Munro A, Brown M, Niblock P, Steele R, Carey F. Do Multidisciplinary Team (MDT) processes influence survival in patients with colorectal cancer? A population-based experience. *BMC Cancer* 2015;15:686.
  26. Zhu S, Chen J, Ni Y, Zhang H, Liu Z, Shen P, et al. Dynamic multidisciplinary team discussions can improve the prognosis of metastatic castration-resistant prostate cancer patients. *Prostate* 2021;81:721-7.
  27. Anderson JM, Rodriguez A, Chang DT. Foreign body reaction to biomaterials. *Semin Immunol* 2008;20:86-100.
  28. Kumar GVS, Ramani S, Mahajan A, Jain N, Sequeira R, Thakur M. Imaging of retained surgical items: A pictorial review including new innovations. *Indian J Radiol Imaging* 2017;27:354-61.

**Cite this article as:** Li Y, He K, Hao X, Morelli JN, Shen Y, Hu X, Hu D, Li Z. Gastrointestinal tumor-related perihepatic fluorouracil encapsulated lesions and liver metastases: a diagnostic imaging study based on contrast-enhanced computed tomography and magnetic resonance imaging. *Quant Imaging Med Surg* 2023;13(10):7236-7246. doi: 10.21037/qims-22-1315

**Table S1** Clinical characteristics of the patients with FELs included for imaging analysis

Item	Number of patients with FELs/mean $\pm$ SD
Total number	33
Age (years)	
Mean $\pm$ SD	55.73 $\pm$ 10.10
Range	30–81
Male (mean $\pm$ SD, range)	55.48 $\pm$ 11.28, 30–81
Female (mean $\pm$ SD, range)	56.50 $\pm$ 5.43, 51–68
Sex (male/female)	25/8
Cancer	
Gastric cancer	28
pTNM	
I	1 (T1N0M0)
II	11 (T3N0M0, T3N1M0, T4aN0M0)
III	16 (T2N3aM0, T3N2M0, T3N3aM0, T4aN3aM0, T4bN2M0)
Colorectal cancer	5
pTNM	
II	4 (T3N0M0, T4N0M0)
III	1 (T2N1M0)

pTNM staging of gastric cancer and colorectal cancer refers to the UICC and AJCC staging system. FEL, fluorouracil encapsulated lesion; SD, standard deviation; pTNM, pathological tumor-node-metastasis; UICC, Union for International Cancer Control; AJCC, American Joint Committee on Cancer.

**Table S2** Tumor types and TNM staging of patients with liver metastases

Type	Number of patients (TNM staging)
Gastric cancer	3
III	1 (pT3N3M0)
IV	2 (pT4N1M1)
Colorectal cancer	24
II	4 (pT3N0M0, ypT3N0M0)
III	8 (pT3N1M0, pT3N2M0, pT4N1M0, pT4N2M0, ypT4N2M0)
IV	12 (cT3N0M1, cT4N2M1, pT3N0M1, pT3N1M1, pT4N0M1, pT4N1M1)
Lung cancer	7
IV	cT2N0M1, cT3N2M1, cT4N0M1, cT4N3M1
Breast cancer	2
II	pT2N0M0, pT2N1M0
Thyroid cancer	1
IV	pTxNxM1
Ampullary cancer	1
IV	pT3N0M1
Gastric stromal tumor	1
IV	pT4N0M1
Cervical cancer	1
II	ypT2N0M0

TNM staging of the cancers mentioned above refers to the UICC and AJCC staging system. Patients with surgical resection are presented with pTNM/ypTNM staging. Patients treated conservatively are presented with cTNM staging at the time of liver metastasis. Due to the incomplete clinical data of the patient with thyroid cancer, we only recorded M staging. TNM, tumor-node-metastasis; pTNM, pathological tumor-node-metastasis; ypTNM, post-neoadjuvant tumor-node-metastasis; cTNM, clinical tumor-node-metastasis; UICC, Union for International Cancer Control; AJCC, American Joint Committee on Cancer.